

# A Closed-Form Spatial Green's Function for the Thick Microstrip Substrate: The Meshless Interpolation Approach

B. Honarbakhsh<sup>1</sup> and A. Tavakoli<sup>2</sup>

<sup>1</sup>Department of Electrical Engineering  
Amirkabir University of Technology (Tehran Polytechnic), Tehran, IRAN  
b\_honarbaksh@aut.ac.ir

<sup>2</sup>Institute of Communications Technology and Applied Electromagnetics  
Amirkabir University of Technology (Tehran Polytechnic), Tehran, IRAN  
tavakoli@aut.ac.ir

**Abstract** — In this paper the Green's functions (GFs) of a thick microstrip in the spatial-domain is computed based on expanding the corresponding spectral-domain functions over inverse quadric (IQ) radial basis functions (RBFs). The scattered data interpolation ability of RBFs is exploited for efficient sampling of the Sommerfeld integration path (SIP), passing from close vicinity of singularities in the complex  $k_p$  plane. By this, the information content of spectral-domain GFs is preserved, which makes it possible to compute the far-fields accurately. Thus, the method can be applied to the analysis of electrically large structures near layered media. The proposed method is direct with only one approximation level.

**Index Terms** - Microstrip, integral equation, IQ, RBF, and Sommerfeld integral.

## I. INTRODUCTION

Development of integral equation (IE)-based methods, was a revolutionary step in the growth of computational electromagnetics (CEM). The most obvious advantage of IE solvers over PDE solvers is to decrease the amount of discretization region, which is limited only to the body under study in the former case. This removes the need of IE solvers to absorbing boundary conditions (ABCs), which is a troubling requirement of PDE counterparts [1, 2]. There also exists a rather not obvious priority for IE solvers, which if not

dismissed, is not sufficiently highlighted in the literature; i.e., *the unambiguous description of the problem at its edges and corners*. To clarify this issue, consider electromagnetic (EM) scattering from a PEC plate. Handling this problem by the Finite Element Method (FEM) requires determination of boundary conditions at interior region of the plate, its edges and corners. Although for the interior region, the tangential components of the electric field are known to be zero, the exact condition on EM fields is unknown on rest of the boundary. What is known is its order of singularity [3]. On the other hand, solving the same problem by MoM is straightforward noting that at the edges, the normal component of current and at the corners, the total current should vanish [4].

Beside the aforementioned benefits, there are two challenges dealing with IE solvers. The first is the knowledge of the Green's function (GF) of the problem, which is known for limited cases such as free space, half-space, and multi-layered media [5]. The second challenge is computing the layered media GF in the spatial-domain, which requires numerical evaluation of an inverse Fourier-Bessel transform (IFBT) and follows four difficulties. First, the spectral-domain GFs are multi-valued, having number of branch point singularities and their corresponding branch cuts. Second, these functions have number of pole singularities, leading to abrupt changes. It is important to note that in addition to poles, which intrinsically lead to harsh variations, some of the branch points also lead to such behavior. Third, the Bessel functions

are oscillatory, which complicates the process of the numerical integration. Fourth, the Bessel functions are slow decaying, which decelerates the computation process, i.e., more sampling is needed, which will lead to longer computation time.

At present, a winning approach to the problem is expanding the spectral-domain GFs over a class of functions with known analytical IFBT. Assuming a successful expansion, all four said difficulties are bypassed. In the recent decades, lots of research is done based on this idea, e.g., [6-13]. These methods can be classified from the following aspects:

#### A. Expansion function

Up to now, the most used expansion functions are complex exponentials [6, 7, 10], rational [8, 11] and Gaussian functions [13], in either of  $k_{z0}$  or  $k_\rho$  complex planes, defined in [6]. These planes can be uniquely mapped on each other. The corresponding integrals are then analytically computed via available mathematical identities, e.g., the Sommerfeld Identity (SI) [5], or by the residue theorem [14].

#### B. Expansion method

Expanding a known function over a class of functions with unknown parameters can be studied under the context of model-based parameter estimation (MBPE). The MBPE can be carried out by non-linear programming or optimization methods. However, there exist conditions which allow solving non-linear problems by linear algebra, e.g., the Prony method [15], generalized pencil-of-function (GPOF) method [16] and matrix-pencil method (MPM) [17]. These methods are all one-step solutions to the expansion problem and expand a complex valued function of a real variable over sum of complex exponentials, provided that the independent variable is sampled uniformly. For expanding over rational functions, the rational function fitting method (RFFM) has currently attracted the researchers [18]. This method is iterative and should be initialized properly.

#### C. Dependence on human labour

Achieving fully automatic IE solver requires direct methods for computation of spatial-domain GFs. By direct method, it is meant methods independent of human labour, e.g., [7, 10]. In the

pioneering works, e.g. [6], the contributions of quasi dynamic images and surface-wave poles (SWPs) were subtracted, analytically. It should be noted that for a general multilayered case, the surface-wave terms cannot be obtained analytically [10].

#### D. Integration path

Another distinguishing factor is the integration path, which is called the Sommerfeld integration path (SIP). The SIP can be considered in either of the  $k_{z0}$  or  $k_\rho$  complex planes. Theoretically, all valid paths are equivalent. However, as clearly stated in [10], the limited number of significant digits in numerical computations leads to different results from different paths. The information content of the evaluated GFs increases as the path become closer to singular points. Thus, if the expansion method is incapable of tracking abrupt changes, the path should pass sufficiently far from singularities. Stating another way, there is a compromise between the sharpness of the function and its information content. Such a decrease, leads to erroneous evaluations in the far-field region of the spatial-domain GFs.

#### E. Number of approximation levels

The variation rate of the spectral-domain GFs differs on different sections of the SIP. Therefore, if the expansion method requires uniform sampling, the efficiency of the process decreases drastically. This fact should specially be considered when direct methods are of interest. A classical solution to this problem is partitioning the integration path to sub-sections and sample each of them independently, based on the behavior of the corresponding spectral-domain GF. The number of approximation levels is then equal to the number of partitions. This procedure is utilized in [7] for the first time, leading to a two-level approximation, and is still followed by other researchers.

#### F. Physical compatibility

Different sections of the SIP correspond to EM waves of different nature. Thus, it seems reasonable to expand each part such that its IFBT coincides with the real nature of the wave. For instance, the EM wave at the near-field and the far-field along the substrate becomes spherical and cylindrical, respectively. Consequently, physical compatibility

is met by expanding the low and high spatial frequency sections of the path such that their IFBT lead to  $e^{-jk_0 r}/r$  and  $H_0^{(1)}(k_0 \rho)$ , respectively, as is done in [11]. Nevertheless, for a successful result, such a compatibility is not necessary [10].

The proposed method employs inverse quadric (IQ) and radial basis functions (RBFs) for expansion, which are rational [19]. The RBFs are mainly constructed for scattered data interpolations [20] and are currently exploited in mesh free solution of operator equations [21, 22]. Expanding over RBFs is done by solving a linear system of equations. Therefore, the expansion process is carried out in one-step, without the need to initial guess. The proposed method is direct and does not need any human labor. Moreover, the extreme ability of RBFs in data fitting makes it possible to pass the SIP from vicinity of singularities. As a result, the method is capable to correctly evaluate the spatial-domain GFs in the far-field region, due to preserving the information content of the spectral-domain GFs. Thus, the method is applicable for the analysis of electrically large structures near layered media. The scattered data interpolation property of RBFs is utilized for non-uniform sampling of the SIP, leading to one-level approximation and significant increase in computational efficiency. Finally, the method does not possess physical compatibility, due to expressing the EM field by cylindrical waves in the whole spatial range.

## II. MATHEMATICAL STATEMENT OF THE PROBLEM

Suppose an infinite grounded dielectric substrate with height  $h$  and real electric permittivity of  $\epsilon_r$ . The substrate is placed on  $x$ - $y$  plane such that its top side coincides with  $z = 0$ . This structure is illuminated by an  $x$ -directed electric dipole of unit strength located at  $z = z' \geq 0$  and oscillating at frequency  $f = f_0$ . It is assumed that  $z \geq 0$  is free space. Under these assumptions, the spatial-domain GFs in the air region can be computed by [6]

$$\begin{cases} G_A^{xx} = \frac{\mu_0}{4\pi} \frac{e^{-jk_0 r_0}}{r_0} + \frac{\mu_0}{4\pi} F(R_{TE}) \\ G_q = \frac{1}{4\pi\epsilon_0} \frac{e^{-jk_0 r_0}}{r_0} + \frac{1}{4\pi\epsilon_0} F(R_{TE} + R_q) \end{cases}, \quad (1)$$

with

$$F(\cdot) = \int_{\text{SIP}} (\cdot) \frac{e^{-jk_0(z+z')}}{jk_{z_0}} J_0(k_\rho \rho) k_\rho dk_\rho, \quad (2)$$

where  $J_0$  is the zero order Bessel function, and

$$\begin{cases} R_{TE} = -\frac{r_{10}^{TE} + \Phi}{1 + r_{10}^{TE} \Phi} \\ R_q = \frac{2k_{z_0}^2 (1 - \epsilon_r)(1 - \Phi^2)}{(k_{z_1} + k_{z_0})(k_{z_1} + \epsilon_r k_{z_0})(1 + r_{10}^{TE} \Phi)(1 - r_{10}^{TM} \Phi)} \end{cases}, \quad (3)$$

with,

$$\begin{cases} r_{10}^{TE} = (k_{z_1} - k_{z_0})(k_{z_1} + k_{z_0})^{-1} \\ r_{10}^{TM} = (k_{z_1} - \epsilon_r k_{z_0})(k_{z_1} + \epsilon_r k_{z_0})^{-1} \\ k_{z_0}^2 + k_\rho^2 = k_0^2 \\ k_{z_1}^2 + k_\rho^2 = \epsilon_r k_0^2 \\ \Phi = \exp(-j2k_{z_1} h) \end{cases}. \quad (4)$$

Traditionally, equation (2) is called the Sommerfeld integral. From the mathematical stand point, equation (2) is an IFBT and SIP coincide the real axis in  $k_\rho$  plane, not passing from poles and branch points [23]. Exclusion of singularities can be theoretically carried out by turning over them with hemi-circles of infinitely small radii such that the path remains in first and third quadrants to satisfy the Sommerfeld radiation condition [5, 23]. Therefore, the integrand remains analytic on the deformed path. It should be noted that the path deformation theorem ensures invariance of the integral [6, 14].

## III. MESHLESS INTERPOLATION BY IQ RBF

Consider the problem of interpolating a function  $u$  based on its  $N$  scattered samples. The samples are assumed to be laid on the real axis, positioned at  $x_1, \dots, x_N$ , and  $u$  is in general, complex valued. Currently, the most famous way for achieving this goal is exploiting RBFs. The RBFs are either global support (GS) or compact support (CS) [22]. There is a fundamental difference between these kinds; the CS RBFs are never analytic whereas it is possible to have analytic GS RBFs.

As a brief description of the proposed method, we intend to evaluate contour integrations over the complex  $k_\rho$ -plane where the integrand is expanded over RBFs. Thus, CS RBFs are excluded and among GS RBFs, the IQ kind is selected because it is analytic, all-pole, and has a well-conditioned

(practically banded and sparse) moment matrix. For the problem at hand, IQ RBF can be expressed as,

$$\varphi(x) = (x^2 + A^2)^{-1} \quad (5)$$

where  $A$  is called the shape parameter [21]. The function  $u$  can now be uniquely interpolated at any  $x \in [x_1, x_N]$ , by the following expansion

$$\begin{cases} u(x) \cong u^h(x) = \sum_{i=1}^N w_i \varphi_i(x) \\ \varphi_i(x) = \varphi(x - x_i) = [(x - x_i)^2 + A_i^2]^{-1}, \end{cases} \quad (6)$$

where  $u^h$  is the interpolated value of  $u$ . In addition,  $A_i$  and  $w_i$  are the shape parameter and weighting of the  $i^{\text{th}}$  sample (node), respectively. The shape parameter can be node dependent. The weightings are simply computed by collocating equation (6) at the nodes and solving a corresponding linear system of equations, which is a well-conditioned diagonal-dominant matrix for the problem at hand.

For determination of the shape parameter, it is preferable to express  $A_i$  as,

$$A_i = \alpha_i d_i, \quad \alpha_i > 0 \quad (7)$$

where  $\alpha_i$  and  $d_i$  are called the dimension less shape parameter and the characteristic length of the  $i^{\text{th}}$  node, respectively [21]. These parameters are, in general, selected empirically. Unless the distribution of samples is not too irregular,  $d_i$  can be selected to be the average nodal spacing [21]. In this work,  $\alpha_i = 2$  and  $d_i = |x_{i+1} - x_i|$ . As a final remark, the IQ RBFs tend to zero outside the sampling region. Thus, if  $u$  is practically zero out of  $[x_1, x_N]$ ,  $u^h$  can also extrapolate it.

#### IV. IQ RBF APPROACH TO THE PROBLEM

In this section, the IQ RBF is used for evaluating equation (2). For this purpose, inspiring from [10], we start with the following SIP

$$\text{SIP}_1 : k_\rho = k'_\rho + j\gamma k_0, \quad 0 \leq k'_\rho < \infty, \quad (8)$$

where  $k'_\rho$  is the real variable of the complex  $k_\rho$  plane and  $\gamma$  is a positive factor. Additionally, let's define

$$\begin{cases} R_1 = \frac{k_\rho}{jk_{z0}} R_{TE} \cdot e^{-jk_{z0}(z+z')} \\ R_2 = \frac{k_\rho}{jk_{z0}} (R_{TE} + R_q) \cdot e^{-jk_{z0}(z+z')} \end{cases}, \quad (9)$$

which leads to the following equivalent statement of equation (2)

$$F_l(\rho) = \int_{\text{SIP}_1} R_l(k_\rho) \cdot J_0(k_\rho \rho) dk_\rho, \quad l=1, 2. \quad (10)$$

The substrate is assumed to be loss-less. Thus, all the singularities of the spectral-domain GFs lay on the real axis and consequently, this path passes from above of  $R_1$  and  $R_2$  singularities. Moreover, since  $\text{SIP}_1$  is a biased version of the real axis, the IQ RBF can interpolate the aforementioned functions based on their samples evaluated on this path. Noting the final remark of the previous section, it is necessary to study the behavior of  $R_1$  and  $R_2$  when  $k_\rho$  approaches to infinity. It is straightforward to show that

$$\begin{cases} \lim_{k_\rho \rightarrow \infty} \text{Re}\{R_1\} = \lim_{k_\rho \rightarrow \infty} \text{Im}\{R_1\} = \lim_{k_\rho \rightarrow \infty} \text{Im}\{R_2\} \\ \lim_{k_\rho \rightarrow \infty} \text{Re}\{R_2\} = (1 - \varepsilon_r)(1 + \varepsilon_r)^{-1} \end{cases}. \quad (11)$$

The above limits can be verified as follows, when  $k_\rho \rightarrow \infty$ , Sommerfeld radiation condition requires  $k_{z0} \rightarrow -j\infty$  and  $k_{z1} \rightarrow -j\infty$ . Therefore,

$$\begin{cases} \Phi \rightarrow 0 \\ r_{10}^{TE} \rightarrow 0 \\ r_{10}^{TM} \rightarrow (1 - \varepsilon_r)(1 + \varepsilon_r)^{-1} \end{cases}. \quad (12)$$

Consequently,

$$\begin{cases} R_{TE} \rightarrow 0 \\ R_q \rightarrow (1 - \varepsilon_r)(1 + \varepsilon_r)^{-1}, \end{cases} \quad (13)$$

which noting to equation (9) leads to equation (11). Thus, interpolating  $R_1$  by IQ RBFs will also lead to its extrapolation. This is not the case for  $R_2$ . One way to overcome this difficulty is to subtract and add the following function from  $R_2$

$$R_b = (1 + \varepsilon_r)(1 - \varepsilon_r)^{-1} \frac{k_\rho}{\sqrt{k_\rho^2 + \eta^2}}, \quad \eta > 0, \quad (14)$$

and rewriting  $R_2$  as:

$$\begin{cases} R_2 = R_3 + R_b \\ R_3 = R_2 - R_b \end{cases}. \quad (15)$$

The function  $R_b$  has the following properties:

$$\begin{cases} \lim_{k_\rho \rightarrow \infty} R_b = (1 - \varepsilon_r)(1 + \varepsilon_r)^{-1} \\ \int_{\text{SIP}_1} R_b \cdot J_0(k_\rho \rho) dk_\rho = (1 - \varepsilon_r)(1 + \varepsilon_r)^{-1} \frac{e^{-\eta \rho}}{\rho}, \end{cases} \quad (16)$$

where the second equality one can be verified by direct application of the SI. The first property in equation (16) ensures automatic extrapolation of  $R_3$  by its expansion over IQ RBFs. In addition, by

the second property in equation (16) the inverse transform of the residual function can be computed analytically. Thus, the problem to be solved simplifies to the evaluation of

$$F_l(\rho) = \int_{\text{SIP}_1} R_l(k_\rho) \cdot J_0(k_\rho \rho) dk_\rho, \quad l=1, 3. \quad (17)$$

For this purpose, consider the following expansion,

$$R^l(k_\rho) \Big|_{\text{SIP}_1} \cong \sum_{i=1}^{N_l} w_i^l \varphi_i^l(k'_\rho), \quad l=1, 3 \quad (18)$$

where  $N_l$  is the number of samples along  $\text{SIP}_1$  for describing  $R_l$  at  $k_{\rho,i}^l, i=1, \dots, N_l$ . Replacing equation (18) into equation (17) and following the final remark of the previous section, the  $\text{SIP}_1$  can be extended to  $\text{SIP}_2$

$$\text{SIP}_2 : k_\rho = \begin{cases} k'_\rho + j\gamma k_0, & 0 \leq k'_\rho < \infty \\ k'_\rho, & -\infty \leq k'_\rho < 0 \end{cases}. \quad (19)$$

This makes it possible to rewrite equation (17) as,

$$F_l(\rho) = \sum_{i=1}^N w_i^l \int_{\text{SIP}_2} \varphi_i^l(k'_\rho) \cdot J_0(k_\rho \rho) dk_\rho, \quad l=1, 3 \quad (20)$$

which by using [23] leads

$$2J_0(z) = H_0^{(1)}(z) - H_0^{(1)}(-z), \quad (21)$$

can be expressed as,

$$F_l(\rho) = F_l^+(\rho) + F_l^-(\rho), \quad l=1, 3 \quad (22)$$

with

$$\begin{cases} F_l^+(\rho) = +\frac{1}{2} \sum_{i=1}^N w_i^l \int_{\text{SIP}_2} \varphi_i^l(k'_\rho) H_0^{(1)}(+k_\rho \rho) dk_\rho \\ F_l^-(\rho) = -\frac{1}{2} \sum_{i=1}^N w_i^l \int_{\text{SIP}_2} \varphi_i^l(k'_\rho) H_0^{(1)}(-k_\rho \rho) dk_\rho \end{cases}, \quad l=1, 3 \quad (23)$$

where  $H_0$  is the zero order Hankel function. At this step, noting that  $H_0^{(1)}(z)$  is analytic at  $+j\infty$ , the integration paths corresponding to  $F_l^+$  and  $F_l^-$  are closed by hemi-circles of infinite radii at upper and lower half planes, respectively. Doing so, equation (23) can be analytically evaluated by direct application of the residue theorem, i.e.,

$$\begin{cases} F_l^+(\rho) = +j\pi \sum_{i=1}^N \frac{w_i^l}{j2A_i^l} H_0^{(1)} \left[ + (k_{\rho,i}^l + jA_i^l) \rho \right] \\ F_l^-(\rho) = -j\pi \sum_{i=1}^N \frac{w_i^l}{j2A_i^l} H_0^{(1)} \left[ - (k_{\rho,i}^l + jA_i^l) \rho \right] \end{cases}, \quad l=1, 3 \quad (24)$$

where  $A_i^l$  is the corresponding shape parameter. This completes the proposed approach of the problem.

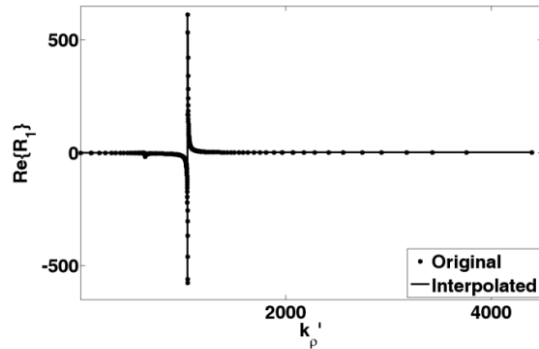
## V. NUMERICAL RESULTS

In this section, the proposed method is applied to a microstrip substrate with  $\epsilon_r = 12.6$  and  $h = 1$  mm illuminated at  $f_0 = 30$  GHz. In addition, it is assumed that  $\gamma = 10^{-3}$ ,  $\eta = 10^2$ ,  $0 \leq k_\rho' \leq 7k_0$  and  $z = z' = 0$ . Using this small value of  $\gamma$ , the information content of singularities are well-preserved and it is expected the method to be able to track the spatial-domain GFs at distances considerably far from the origin. Under the above conditions, the corresponding  $R_l$  and  $R_3$  functions are interpolated based on their non-uniform samples, depicted in Fig. 1. For this purpose, a simple algorithm is developed, which its details are beyond the scope of the paper. As a brief description, the algorithm starts with dividing the domain of the function to number of sub-intervals. Then, it iteratively increases the number of samples in each sub-interval, uniformly, unless the error in the corresponding sub-interval becomes less than a predetermined value. The non-uniform sampling has decreased the number of sample from 8887 to 406 for  $R_l$ , and from 9678 to 1232 for  $R_3$ , which corresponds to the reduction ratio of 95.4 % and 87.3 %, respectively. For clearly demonstrating the capability of IQ RBFs in tracking harsh variations, the singular regions of the functions are enlarged and depicted in Fig. 2. Applying the proposed method to IQ interpolation of  $R_l$  and  $R_3$ , the amplitude of  $G_A^{xx}$  and  $G_q$  functions are evaluated and compared to their corresponding exact values in Figs. 3 (a) and (b), respectively. By exact value, we mean the value computed by direct numerical integration. For better showing the accuracy of the proposed method, the oscillating part of  $G_q$  is enlarged and depicted in Fig. 3 (c). Finally, the effect of  $\gamma$  is studied on  $G_A^{xx}$  and reported in Fig. 4. As is clear and was predictable, the valid range of far-field increases as  $\gamma$  decreases.

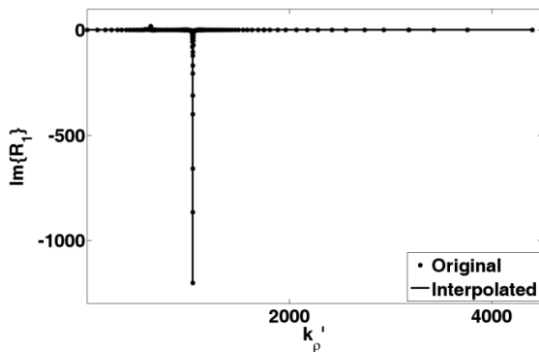
## VI. CONCLUSION

The IQ RBFs are used for expanding the spectral-domain GFs of a microstrip thick substrate. The Sommerfeld integrals corresponding to spatial-domain GFs are then analytically evaluated by the residue theorem. This led to representing electromagnetic fields only by cylindrical waves. In view of extreme capability of

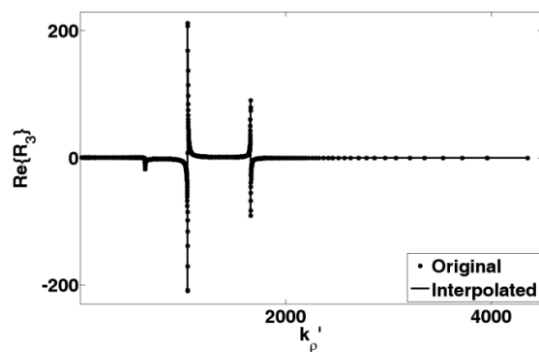
RBFs in data fitting, the SIP is deformed to pass from vicinity of singularities of spectral-domain GFs in the complex  $k_p$ -plane, which led to accurate evaluation of far-fields up to  $\log_{10}(k_0\rho) = 3$ . Moreover, the scattered data interpolation ability of RBFs is utilized for non-uniform sampling of the SIP which has led to considerable increase in computational efficiency.



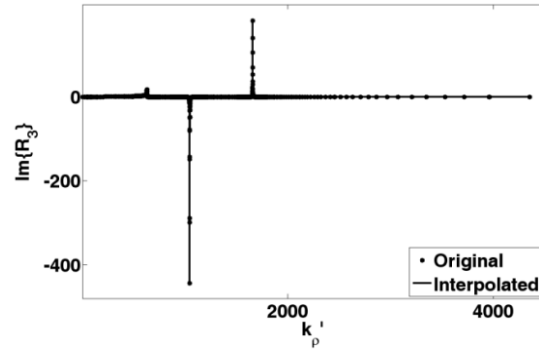
(a)



(b)

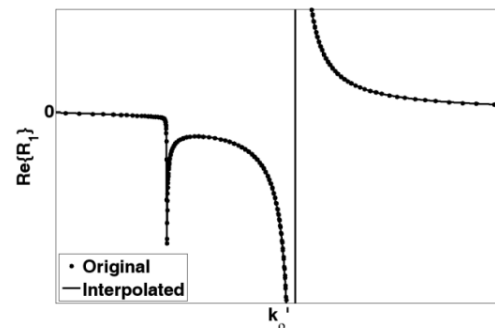


(c)

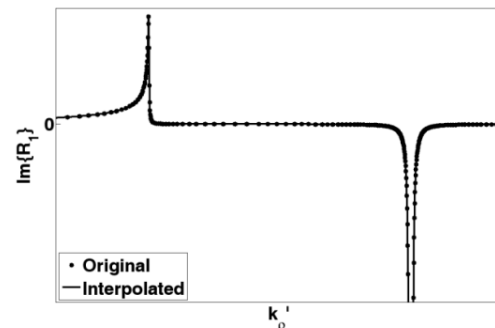


(d)

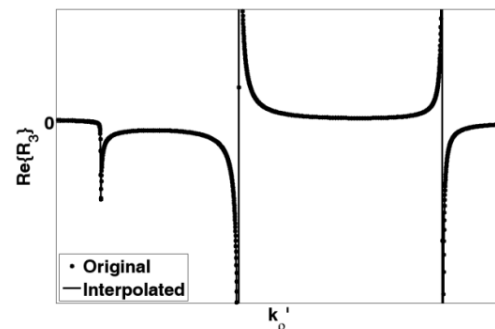
Fig. 1. IQ interpolation of  $R_1$  and  $R_3$  for (a)  $\text{Re}\{R_1\}$ , (b)  $\text{Im}\{R_1\}$ , (c)  $\text{Re}\{R_3\}$ , and (d)  $\text{Im}\{R_3\}$ .



(a)



(b)



(c)

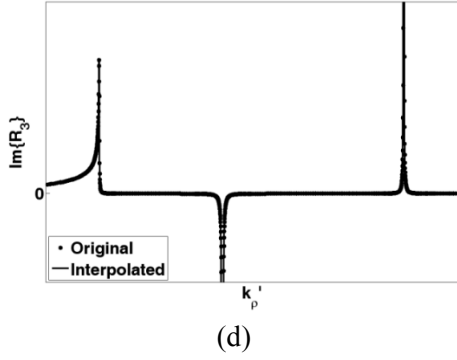


Fig. 2. IQ interpolation of  $R_1$  and  $R_3$ , enlarged at singular regions for (a)  $\text{Re}\{R_1\}$ , (b)  $\text{Im}\{R_1\}$ , (c)  $\text{Re}\{R_3\}$ , and (d)  $\text{Im}\{R_3\}$ .

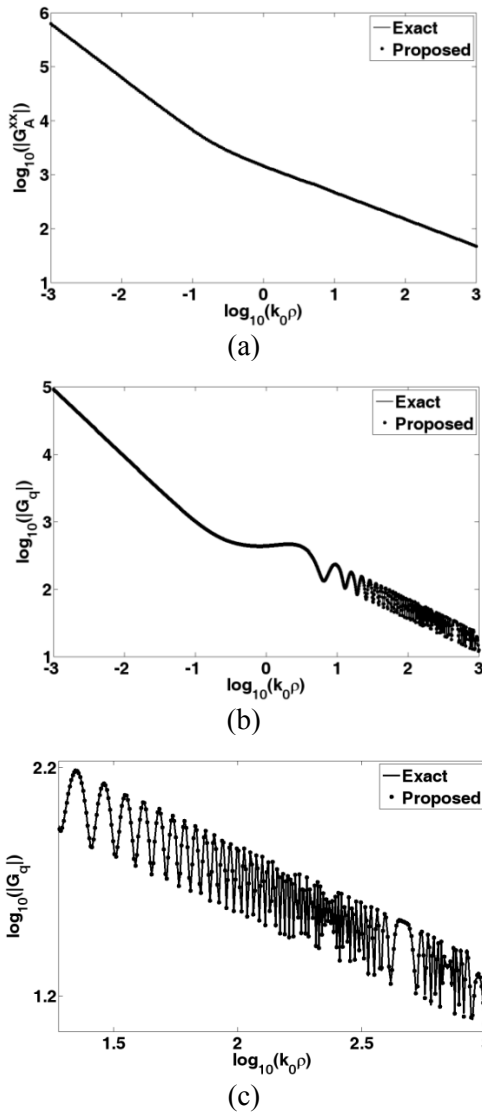


Fig. 3. The amplitude of spatial-domain GFs for (a)  $G_A^{xx}$ , (b)  $G_q$ , (c)  $G_q$  enlarged at its oscillating part.

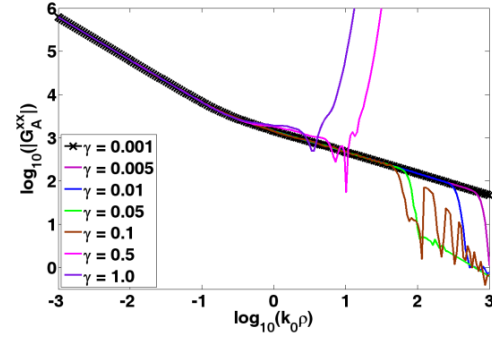


Fig. 4. Effect of  $\gamma$  on  $G_A^{xx}$ .

### ACKNOWLEDGMENT

The authors acknowledge Dr. A. H. Shoory for inputs in Green's function of multilayered media. The authors thank reviewers for many constructive comments.

### REFERENCES

- [1] A. Taflov and S. Hagness, *Computational Electrodynamics*, Third Edition. Artech House, 2005.
- [2] J. Jin, *The Finite Element Method in Electromagnetics*, 2<sup>nd</sup> John Wiley & Sons, 2002.
- [3] J. G. Van Bladel, *Singular Electromagnetic Fields and Sources*. Wiley-IEEE Press, 1996.
- [4] R. Bancroft, *Understanding Electromagnetic Scattering Using the Moment Method*. Artech House, 1996.
- [5] W. C. Chew, *Waves and Fields in Inhomogeneous Media*. IEEE Press, 1995.
- [6] Y. L. Chow, J. J. Yang, D. G. Fang, and G. E. Howard, "A closed-form spatial Green's function for the thick microstrip substrate," *IEEE Trans. Microwave Theory Tech.*, vol. 39, no. 3, pp. 588-592, 1991.
- [7] M. I. Aksun, "A robust approach for the derivation of closed-form Green's functions," *IEEE Trans. Microwave Theory Tech.*, vol. 44, no. 5, pp. 651-658, 1996.
- [8] F. Ling and J. Jin, "Discrete complex image method for Green's functions of general multilayer media," *IEEE Microwave and Guided Wave Letters*, vol. 10, no. 10, pp. 400-402, 2000.
- [9] Y. Ge and K. P. Esselle, "New closed-form Green's functions for microstrip structures theory and results," *IEEE Trans. Microwave Theory Tech.*, vol. 50, no. 6, pp. 1556-1560, 2002.
- [10] M. Yuan, T. K. Sarkar, and M. Salazar-Palma, "A direct discrete complex image method from the closed-form Green's functions in multilayered media," *IEEE Trans. Microwave Theory Tech.*, vol. 54, no. 3, pp. 1025-1032, 2006.

- [11] V. N. Kourkoulos and A. C. Cangellaris, "Accurate approximation of Green's functions in planar stratified media in terms of a finite sum of spherical and cylindrical waves," *IEEE Trans. Antennas Propag.*, vol. 54, no. 5, pp. 1568-1576, 2006.
- [12] A. G. Polimeridis, T. V. Yioultsis, and T. D. Tsiboukis, "A robust method for the computation of Green's functions in stratified media," *IEEE Trans. Microwave Theory Tech.*, vol. 55, no. 7, pp. 1963-1969, 2007.
- [13] M. M. Tajdini and A. A. Shishegar, "A novel analysis of microstrip structures using the Gaussian Green's function method," *IEEE Trans. Antennas Propag.*, vol. 58, no. 1, pp. 88-94, 2010.
- [14] J. W. Brown, R. V. Churchill, *Complex Variables and Applications*. McGraw-Hill, 1996.
- [15] R. W. Hamming, *Numerical Methods for Scientists and Engineers*. Dover Publications, 1987.
- [16] Y. Hua and T. K. Sarkar, "Generalized pencil-of-function method for extracting poles of an EM system from its transient response," *IEEE Trans. Antennas. Propag.*, vol. 37, no. 2, pp. 229-234, 1989.
- [17] T. K. Sarkar and O. Pereira, "Using the matrix pencil method to estimate the parameters of a sum of complex exponentials," *IEEE Antennas Propag. Mag.*, vol. 37, no. 3, pp. 48-55, 1995.
- [18] B. Gustavsen and A. Semlyen, "Rational approximation of frequency domain responses by vector fitting," *IEEE Trans. Power Delivery*, vol. 14, no. 3, pp. 1052-1061, 1999.
- [19] B. Fornberg and C. Piret, "On choosing a radial basis function and a shape parameter when solving a convective PDE on a sphere," *Elsevier J. Comput. Phys.*, vol. 227, pp. 2758-2780, 2008.
- [20] M. J. D. Powell. "The theory of radial basis function approximations in 1990," *Advances in Numerical Analysis: Wavelets, Subdivision Algorithms, and Radial Basis Functions*, vol. 2. W. Light, Ed. USA: Oxford University Press, pp.105-210, 1992.
- [21] G. R. Liu, *Mesh Free Methods*. CRC Press, 2003.
- [22] G. R. Liu and Y. T. Gu, *An Introduction to MeshFree Methods and Their Programming*, Springer, 2005.
- [23] A. Banos, *Dipole Radiation in the Presence of a Conducting Half-Space*, Pergamon, 1966.



**Babak Honarbakhsh** was born in Tehran, Iran. He received his B.Sc. and M.Sc. degrees in Electrical Engineering from Amirkabir University of Technology where he is currently working toward his Ph.D. degree. His current research interest is numerical solution of electromagnetic problems by meshfree methods.



**Ahad Tavakoli** was born in Tehran, Iran, on March 8, 1959. He received B.Sc. and M.Sc. degrees from the University of Kansas, Lawrence, and the Ph.D. degree from the University of Michigan, Ann Arbor, all in electrical engineering, in 1982, 1984, and 1991, respectively. He is currently a Professor in the Department of Electrical Engineering at Amirkabir University of Technology. His research interests include EMC, scattering of electromagnetic waves and microstrip antennas.